Unsteady Subsonic Collocation Method for Wings with and without Control Surfaces

ATLEE M. CUNNINGHAM JR.*
General Dynamics Corporation, Convair Aerospace Division, Fort Worth, Texas

A collocation method is presented for determining aerodynamic loadings on arbitrary planar wings with control surfaces in oscillatory subsonic flow. Functions that are applicable to oscillating full or partial span control surfaces on either the leading or trailing edge are presented. Techniques for treating the kernel function singularities are then applied to the integration of the control surface pressure functions. Rules developed for steady flow are used to determine optimum sets of excess integration points and downwash point arrays. The method is finally verified through comparison with other theories and experiment for several wings with control surfaces. The method is shown to be more efficient than finite element methods.

Nomenclature

a_{nm} = assumed pressure series coefficients
b_0 = root semichord
$b(\eta)$ = semichord at span station η
J = number of integration points per chord
k = $\omega b_0,/U_\infty$ reduced frequency
$\mathbf{K}(x-\xi, Y-\eta, k, M)$ = subsonic oscillatory kernel function
M = freestream Mach number
$NC = \bar{m}$ = downwash points per chord
$NS = \bar{n}$ = downwash chords per semispan
$\mathbf{R}^2$ = $(\tilde{x}-\tilde{\xi})^2 + \beta^2(\tilde{y}-\tilde{\eta})^2$
s_0 = semispan
S = total integration chords (from tip to tip)
U_∞ = freestream velocity
$U_n(\eta)$ = Tschebychev polynomial of the second kind
$\Delta\bar{p}(\xi,\eta)$ = pressure difference amplitude at point ξ,η
$\Delta\bar{p}_R(\xi,\eta)$ = pressure functions for planar surfaces
$\Delta\bar{p}_{cs}(\xi,\eta)$ = pressure functions for control surface displacement
$\bar{w}(x,y)$ = downwash amplitude at point x,y
$\mathbf{W}(x,y)$ = $4\pi\rho U_\infty \bar{w}(x,y)$
x,y = downwash point location
ξ,η = integration point location
$\tilde{x},\tilde{y};\tilde{\xi},\tilde{\eta}$ = $\left(\frac{x}{b_0}\right), \left(\frac{y}{b_0}\right); \left(\frac{\xi}{b_0}\right), \left(\frac{\eta}{b_0}\right)$
$\underline{x},\underline{y};\underline{\xi},\underline{\eta}$ = $\left[\frac{x-x_m(y)}{b(y)}\right], \left(\frac{y}{s_0}\right); \left[\frac{\xi-\xi_m(\eta)}{b(\eta)}\right], \left(\frac{\eta}{s_0}\right)$
$x_m(y),\xi_m(\eta)$ = mid-chord location at span stations y and η, respectively
ρ = freestream density
β^2 = $1-M^2$

Introduction

THE principle equation in oscillatory subsonic lifting surface theory is the integral equation that relates the pressure difference amplitude over the wing surface with the normal velocity or downwash amplitude produced by the surface. This equation may be expressed as

$$\bar{w}(x,y) = \frac{1}{4\pi\rho U_\infty} \iint_{S_w} \Delta\bar{p}(\xi,\eta)\mathbf{K}(x-\xi, y-\eta, k, M)d\xi d\eta \quad (1)$$

where the pressure difference (or lift) amplitude $\Delta\bar{p}(\xi,\eta)$ is unknown. The downwash $\bar{w}(x,y)$ is the sum of the normal velocity induced by the surface slope and that due to normal surface motion at point x,y. The kernel function $\mathbf{K}(x-\xi, y-\eta, k, M)$ is a function of position relative to x,y, reduced frequency, and Mach number M.

In order to obtain a solution to Eq. (1), one may use either an assumed solution with unknown coefficients (collocation method)[1,2,3,4] or finite aerodynamic elements (doublet lattice).[5] The principal disadvantages of the collocation approach are the necessities of choosing appropriate pressure functions and evaluating complicated integrals. On the other hand, finite element methods usually require far more unknown quantities to achieve an adequate solution, and hence, require more computational effort. The advantages and disadvantages of each are discussed by Stark[6] and Cunningham,[3,7] where it was concluded that, for planar surfaces the collocation approach will yield more efficient solutions if the computational time per unknown quantity is about the same for each method.

The collocation method of Hsu[1] essentially achieves the computational efficiency of the finite element methods through the use of Gaussian quadrature integration. In Hsu's method, the number of integration points per semispan are only slightly larger than the number of control points per semi-span. The method does contain instabilities as is discussed by Rowe[2] who found that by increasing the number of integration points, a stable solution could be achieved. This diminished the efficiency of the method and, hence, is an unattractive solution to the problem. An improved version of the method has been developed[3,7,8] whereby stable solutions are achieved without resorting to excess integration points.

This paper presents a summary of the new development of Hsu's method for unsteady flow and the extension to include wings with control surfaces. A more accurate quadrature integration formula is presented that accounts for all of the singularities of the kernel function. The results of the development of the steady flow method[7] are extended to unsteady flow and wings with control surfaces. This allows determination, a priori, of appropriate downwash point arrays based on planform geometry and Mach number, which will produce a solution of acceptable accuracy. The control surface extension is basically that for which some preliminary results have already been presented.[3] The pressure function

Presented at the AIAA/ASME 11th Structures, Structural Dynamics and Materials Conference, Denver, Colo., April 22–24, 1970; submitted July 6, 1970; revision received January 26, 1972. Sponsored by the Convair Aerospace Division of General Dynamics in an independent research and development program.

Index categories: Aeroelasticity and Hydroelasticity; Structural Dynamic Analysis; Airplane and Component Aerodynamics.

* Senior Structures Engineer, Associate Fellow AIAA.

is the same; however, the integration technique has been refined such that accurate integrals may be obtained without the use of excess integration points.

Integral Equation for Planar Surfaces

Following Hsu,[1] Eq. (1) may be written with the essential singularities broken out as follows:

$$\overline{\mathbf{W}}_R(\tilde{x},\tilde{y}) = \frac{1}{s_0}\int_{-1}^{1}\frac{\partial}{\partial\underline{\eta}}\left\{\int_{-1}^{1}\Delta\bar{p}_R(\underline{\xi},\underline{\eta})e^{-ik(\tilde{x}-\tilde{\xi})}\times\left[1+\frac{\tilde{x}-\tilde{\xi}}{\mathbf{R}}\right]b(\underline{\eta})d\underline{\xi}\right\}\frac{d\underline{\eta}}{\underline{y}-\underline{\eta}} + \left(\frac{s_0}{b_0}\right)^2\int_{-1}^{1}\int_{-1}^{1}\Delta\bar{p}_R(\underline{\xi},\underline{\eta})e^{-ik(\tilde{x}-\tilde{\xi})}\times\left[\frac{ik}{\mathbf{R}}-\frac{k^2}{2}\ln|\mathbf{R}-(\tilde{x}-\tilde{\xi})|+H(\tilde{x}-\tilde{\xi},\tilde{y}-\tilde{\eta})\right]b(\underline{\eta})d\underline{\xi}d\underline{\eta} \quad (2)$$

(For term definition see Nomenclature and for coordinate system relationships see Fig. 1.) The pressure distribution for planar surfaces is assumed as

$$\Delta\bar{p}_R(\underline{\xi},\underline{\eta}) = \frac{4\rho U_\infty{}^2}{b(\underline{\eta})}s_0(1-\underline{\eta}^2)^{1/2}\times\left[g_0(\underline{\eta})\left(\frac{1-\underline{\xi}}{1+\underline{\xi}}\right)^{1/2}+g_1(\underline{\eta})(1-\underline{\xi}^2)^{1/2}+g_2(\underline{\eta})\underline{\xi}(1-\underline{\xi}^2)^{1/2}+\cdots\right] \quad (3a)$$

where

$$g_n(\underline{\eta}) = a_{n0}U_0(\underline{\eta})+a_{n1}U_1(\underline{\eta})+a_{n2}U_2(\underline{\eta})+\cdots \quad (3b)$$

and $U_m(\underline{\eta})$ are the Tschebychev polynomials of the second kind. Inserting Eq. (3) into (2), the working form of the equation becomes

$$\frac{\overline{\mathbf{W}}_R(\tilde{x},\tilde{y})}{4\rho U_\infty{}^2} = W_{R1}(\tilde{x},\tilde{y})+W_{R2}(\tilde{x},\tilde{y})+W_{R3}(\tilde{x},\tilde{y})+W_{R4}(\tilde{x},\tilde{y}) \quad (4)$$

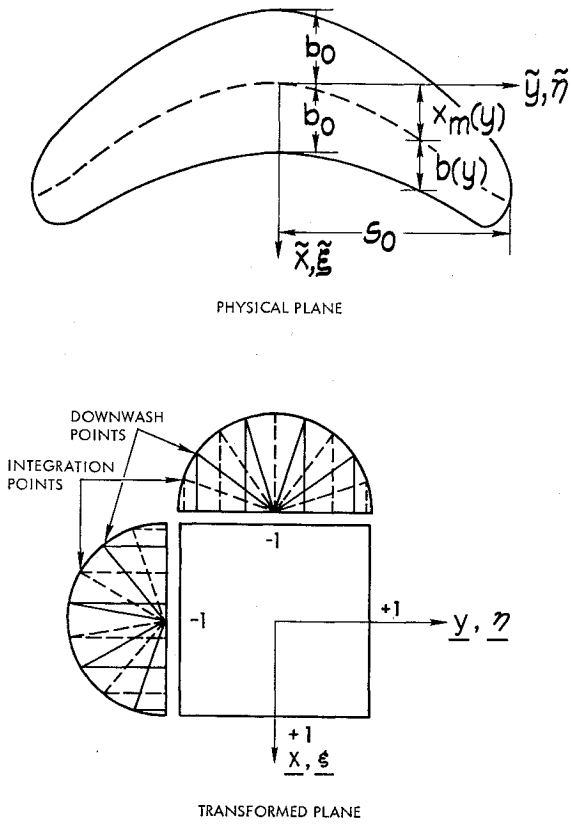

Fig. 1 Arbitrary planform in physical and transformed plane.

where

$$W_{R1}(\tilde{x},\tilde{y}) = \int_{-1}^{1}\frac{\partial}{\partial\underline{\eta}}\left\{(1-\underline{\eta}^2)^{1/2}\int_{-1}^{1}\Phi_R(\underline{\xi},\underline{\eta})\times\left[1+\frac{\tilde{x}-\tilde{\xi}}{\mathbf{R}}\right]d\underline{\xi}\right\}\frac{d\underline{\eta}}{\underline{y}-\underline{\eta}} \quad (5a)$$

$$W_{R2}(\tilde{x},\tilde{y}) = ik\left(\frac{s_0}{b_0}\right)^2\int_{-1}^{1}\int_{-1}^{1}(1-\underline{\eta}^2)^{1/2}\Phi_R(\underline{\xi},\underline{\eta})\frac{d\underline{\xi}d\underline{\eta}}{\mathbf{R}} \quad (5b)$$

$$W_{R3}(\tilde{x},\tilde{y}) = -\frac{k^2}{2}\left(\frac{s_0}{b_0}\right)^2\int_{-1}^{1}\int_{-1}^{1}(1-\underline{\eta}^2)^{1/2}\Phi_R(\underline{\xi},\underline{\eta})\times\ln|\mathbf{R}-(\tilde{x}-\tilde{\xi})|d\underline{\xi}d\underline{\eta} \quad (5c)$$

$$W_{R4}(\tilde{x},\tilde{y}) = \left(\frac{s_0}{b_0}\right)^2\int_{-1}^{1}\int_{-1}^{1}(1-\underline{\eta}^2)^{1/2}\Phi_R(\underline{\xi},\underline{\eta})\times H(\tilde{x}-\tilde{\xi},\tilde{y}-\tilde{\eta})d\underline{\xi}d\underline{\eta} \quad (5d)$$

and

$$\Phi_R(\underline{\xi},\underline{\eta}) = \left[g_0(\underline{\eta})\left(\frac{1-\underline{\xi}}{1+\underline{\xi}}\right)^{1/2}+g_1(\underline{\eta})(1-\underline{\xi}^2)^{1/2}+\cdots\right]e^{-ik(\tilde{x}-\tilde{\xi})} \quad (5e)$$

The first equation is almost identical with the equation for steady flow with exception of the exponential term in $\Phi_R(\underline{\xi},\underline{\eta})$. Its treatment will make use of this similarity and, hence, that development in Ref. 7. The next two equations represent different singularities and thus require different treatment as was shown in Ref. 3. The last equation may be evaluated directly with quadrature integration formulas since $H(\tilde{x}-\tilde{\xi},\tilde{y}-\tilde{\eta})$ is a smooth and continuous function. The detailed derivations of these equations are presented in Ref. 8.

Integration of the Equation for Planar Surfaces

In this section the final form of the equations for planar wings will be presented. Since the derivations have been previously published,[3,8] they will not be repeated in this paper. With exception of a correction [Eq. (11b) in Ref. 3] and a slight modification to the correction term for Eq. (5a), the following equations are as presented previously.

The complete integration formula may be written as a double summation for the downwash at point $(\tilde{x}_i,\tilde{y}_r)$ as

$$\frac{\overline{\mathbf{W}}_R(\tilde{x}_i,\tilde{y}_r)}{4\rho U_\infty{}^2} = \frac{2\pi^2}{S(2J+1)}\sum_{s=1}^{S}\sum_{j=1}^{J}(1-\underline{\eta}_s{}^2)[g_0(\underline{\eta}_s)(1-\underline{\xi}_j)+g_1(\underline{\eta}_s)(1-\underline{\xi}_j{}^2)+\cdots]\mathbf{K}(\tilde{x}_i-\tilde{\xi}_j,\tilde{y}_r-\tilde{\eta}_s,k,M)+\frac{2\pi^2 S}{2J+1}\sum_{j=1}^{J}[g_0(\underline{y}_r)(1-\underline{\xi}_j)+g_1(\underline{y}_r)(1-\underline{\xi}_j{}^2)+\cdots]\left[1+\frac{|\underline{x}_i-\underline{\xi}_j|}{\underline{x}_i-\underline{\xi}_j}\right]\exp\left[-ik\frac{b(\underline{y}_r)}{b_0}(\underline{x}_i-\underline{\xi}_j)\right]+\left[-\frac{\pi}{S}\sum_{s=1}^{S}\frac{(1-\underline{\eta}_s{}^2)}{(\underline{y}_r-\underline{\eta}_s)^2}\Psi_{GR}(\underline{y}_r,\underline{\eta}_s)+\pi S\Psi_{GR}(\underline{y}_r,\underline{y}_r)+ik\left(\frac{s_0}{b_0}\right)^2\Phi_R(\underline{x}_i,\underline{y}_r)\Gamma(\tilde{x}_i,\tilde{y}_r)-\frac{k^2}{2}\left(\frac{s_0}{b_0}\right)^2\frac{2\pi}{2S+1}\sum_{j=1}^{J}\Omega_R(\underline{\xi}_j,\underline{y}_r)\right] \quad (6)$$

The kernel function is

$$\mathbf{K}(\tilde{x}_i-\tilde{\xi}_j,\tilde{y}_r-\tilde{\eta}_s,k,M) = \left(\frac{s_0}{b_0}\right)^2\left\{\frac{-1}{(\tilde{y}_r-\tilde{\eta}_s)^2}\left[1+\frac{\tilde{x}_i-\tilde{\xi}_j}{\mathbf{R}_{ij,rs}}\right]+\frac{ik}{\mathbf{R}_{ij,rs}}-\frac{k^2}{2}\ln|\mathbf{R}_{ij,rs}-(\tilde{x}_i-\tilde{\xi}_j)|+H(\tilde{x}_i-\tilde{\xi}_j,\tilde{y}_r-\tilde{\eta}_s)\right\}e^{-ik(\tilde{x}_i-\tilde{\xi}_j)} \quad (7)$$

which is identical to that given by Watkins, Runyan and Woolston.[9] The functions $\Psi_{GR}(\underline{y}_r, \underline{\eta}_s)$, $\Gamma(\tilde{x}_i, \tilde{y}_r)$ and $\Omega_R(\underline{\xi}_j, \underline{y}_r)$ are the correction terms that account for the various singularities and discontinuities in Eqs. (5a–5d).

The first correction term accounts for the chordwise discontinuity in the kernel function and is given here in a slightly modified form as

$$\Psi_{GR}(\underline{y}_r, \underline{\eta}_s) = \sum_{p=0}^{1} (-1)^p \Phi_{Rp(x)}(\underline{x}_i, \underline{\eta}_s)\psi_{Rp}(\tilde{y}_r, \tilde{\eta}_s) \tag{7a}$$

where

$$\Phi_{Rp(x)}(\underline{x},\underline{\eta}) = \left[\frac{\partial^p}{\partial \underline{\xi}_p} \Phi_R(\underline{\xi},\underline{\eta})\right]_{\underline{x},\underline{\eta}}$$

or

$$\Phi_{R0}(\underline{x},\underline{\eta}) = \left[g_0(\underline{\eta})\left(\frac{1-\underline{x}}{1+\underline{x}}\right)^{1/2} + g_1(\underline{\eta})(1-\underline{x}^2)^{1/2} + \cdots\right] \tag{7b}$$

$$\Phi_{R1}(\underline{x},\underline{\eta}) = \frac{d}{d\underline{x}}\left[g_0(\underline{\eta})\left(\frac{1-\underline{x}}{1+\underline{x}}\right)^{1/2} + g_1(\underline{\eta})(1-\underline{x}^2)^{1/2} + \cdots\right] + kb(\underline{\eta})\Phi_{R0}(\underline{x},\underline{\eta}) \tag{7c}$$

and

$$\psi_{R0}(\tilde{y},\tilde{\eta}) = \frac{1}{2}\left\{\mathbf{H}_0(\tilde{y},\tilde{\eta}) - \frac{2\pi}{2J+1}\sum_{j=1}^{J}(1-\underline{\xi}_j^2)^{1/2} \times \left[1 + \frac{\tilde{x}-\tilde{\xi}_j}{[(\tilde{x}-\tilde{\xi}_j)^2 + \beta^2(\tilde{y}-\tilde{\eta})^2]^{1/2}}\right]\right\} \tag{7d}$$

$$\psi_{R1}(\tilde{y},\tilde{\eta}) = \left[\frac{\tilde{x}-\tilde{\xi}_{le}(\tilde{\eta})}{b(\tilde{\eta})} - (1+\underline{x})\right]\psi_{R0}(\tilde{y},\tilde{\eta}) + \frac{1}{2b(\tilde{\eta})}\left\{\mathbf{H}_1(\tilde{y},\tilde{\eta}) - \frac{2\pi}{2J+1}\sum_{j=1}^{J}(1-\underline{\xi}_j^2)^{1/2}(\tilde{x}-\tilde{\xi}_j) \times \left[1 + \frac{\tilde{x}-\tilde{\xi}_j}{[(\tilde{x}-\tilde{\xi}_j)^2 + \beta^2(\tilde{y}-\tilde{\eta})^2]^{1/2}}\right]\right\} \tag{7e}$$

The $\mathbf{H}_p(\tilde{y},\tilde{\eta})$ terms are the analytic integrals of the essential discontinuities

$$\mathbf{H}_0(\tilde{y},\tilde{\eta}) = 2 + \frac{1}{b(\tilde{\eta})}\{[(\tilde{x}-\tilde{\xi}_{le}(\tilde{\eta}))^2 + \beta^2(\tilde{y}-\tilde{\eta})^2]^{1/2} - [(\tilde{x}-\tilde{\xi}_{te}(\tilde{\eta}))^2 + \beta^2(\tilde{y}-\tilde{\eta})^2]^{1/2}\} \tag{7f}$$

$$\mathbf{H}_1(\tilde{y},\tilde{\eta}) = \frac{-1}{2b(\tilde{\eta})}\{[\tilde{x}-\tilde{\xi}_{le}(\tilde{\eta})]^2 - [\tilde{\xi}_{te}(\tilde{\eta})-\tilde{x}]^2 + [\tilde{x}-\tilde{\xi}_{le}(\tilde{\eta})][(\tilde{x}-\tilde{\xi}_{le}(\tilde{\eta}))^2 + \beta^2(\tilde{y}-\tilde{\eta})^2]^{1/2} + [\tilde{\xi}_{te}(\tilde{\eta})-\tilde{x}][(\tilde{\xi}_{te}(\tilde{\eta})-\tilde{x})^2 + \beta^2(\tilde{y}-\tilde{\eta})^2]^{1/2} - \beta^2(\tilde{y}-\tilde{\eta})^2 \ln\left|\frac{[(\tilde{x}-\tilde{\xi}_{le}(\tilde{\eta}))^2 + \beta^2(\tilde{y}-\tilde{\eta})^2]^{1/2} + [\tilde{x}-\tilde{\xi}_{le}(\tilde{\eta})]}{[(\tilde{\xi}_{te}(\tilde{\eta})-\tilde{x})^2 + \beta^2(\tilde{y}-\tilde{\eta})^2]^{1/2} - [\tilde{\xi}_{te}(\tilde{\eta})-\tilde{x}]}\right|\} \tag{7g}$$

The terms $\tilde{\xi}_{le}(\tilde{\eta})$ and $\tilde{\xi}_{te}(\tilde{\eta})$ are the leading and trailing edge coordinates, respectively, in the physical coordinate system at the station $\tilde{\eta}$. The preceding form for the discontinuity correction term provides a better representation for swept surfaces near the leading edge as opposed to the earlier version.[3,8]

The second correction term accounts for the point singularity in Eq. (5b) at the downwash point and is given as

$$\Gamma(\tilde{x}_i,\tilde{y}_r) = \mathbf{F}(\tilde{x}_i,\tilde{y}_r) - \frac{2\pi^2}{S(2J+1)}\sum_{s=1}^{S}\sum_{j=1}^{J}\frac{(1-\underline{\eta}_s^2)(1-\underline{\xi}_j^2)^{1/2}}{\mathbf{R}_{ij,rs}} \tag{8a}$$

where

$$\mathbf{F}(\tilde{x},\tilde{y}) = \frac{\pi}{S}\sum_{s=1}^{S}(1-\underline{\eta}_s^2)\left[D(\underline{x},\underline{\eta}_s) - \frac{2b_0}{b(\underline{\eta}_s)}\ln|1+\delta(\underline{\eta}_s)\underline{y}|\right] - 2b_0\sum_{m=1}^{M}H_m\left\{\frac{(1+\underline{y})(1-\underline{y}_+^2)^{1/2}}{b(\underline{y}_+)} + \frac{(1-\underline{y})(1-\underline{y}_-^2)^{1/2}}{b(\underline{y}_-)}\right\} \tag{8b}$$

and

$$D(\underline{x},\underline{\eta}) = \frac{b_0}{b(\underline{\eta})}\ln\left|\left(\frac{s_0}{b_0\beta}\right)^2\{[(\tilde{x}-\tilde{\xi}_{le}(\tilde{\eta}))^2 + \beta^2(\tilde{y}-\tilde{\eta})^2]^{1/2} + [\tilde{x}-\tilde{\xi}_{le}(\tilde{\eta})]\}\cdot\{[(\tilde{\xi}_{te}(\tilde{\eta})-\tilde{x})^2 + \beta^2(\tilde{y}-\tilde{\eta})^2]^{1/2} + [\tilde{\xi}_{te}(\tilde{\eta})-\tilde{x}]\}\right| \tag{8c}$$

$$\delta(\underline{\eta}) = \begin{cases} +1, & \underline{\eta} \le \underline{y} \\ -1, & \underline{\eta} > \underline{y} \end{cases} \tag{8d}$$

$$\underline{y}_+ = \underline{y} - a_m(1+\underline{y}) \tag{8e}$$

$$\underline{y}_- = \underline{y} - a_m(1-\underline{y}) \tag{8f}$$

The chordwise integration of Eq. (5b) is performed first, which results in a spanwise logarithmic singularity. It is convenient to perform quadrature integration of this singularity with the following formula

$$\int_0^1 f(x)\ln(x)dx = \sum_{m=1}^{\bar{M}} H_m f(a_m) \tag{9}$$

where the H_m and a_m are available.[10] Although other logarithmic singularities must be integrated in this method, it is not convenient to use Eq. (9), thus other approaches are taken.

The third correction term accounts for the spanwise logarithmic singularity in Eq. (5c) and is given as

$$\Omega_R(\underline{\xi}_j,\underline{y}_r) = \sum_{p=0}^{1}\left\{\frac{\partial^p}{\partial\underline{\eta}^p}[g_0(\underline{\eta})(1-\underline{\xi}_j) + g_1(\underline{\eta})(1-\underline{\xi}_j^2) + \cdots]\right\}_{\underline{\eta}=\underline{y}_r} e^{-ik(\tilde{x}_i-\tilde{\xi}_j)}\left[\mathbf{I}_p(\underline{\xi}_j,\underline{y}_r) - \frac{\pi}{S}\sum_{s=1}^{S}(1-\underline{\eta}_s^2)^{1/2}(\underline{\eta}_s-\underline{y}_r)^p \times \ln|\mathbf{R}_{ij,rs} - (\tilde{x}_i-\tilde{\xi}_j)|\right] \tag{10a}$$

where

$$\mathbf{I}_0(\underline{\xi}_j,\underline{y}_r) = -2 + (1+\underline{y}_r)\ln|(\mathbf{R}_{ij,r})_2 - (\tilde{x}_i-\tilde{\xi}_j)| + (1-\underline{y}_r)\ln|(\mathbf{R}_{ij,r})_1 - (\tilde{x}_i-\tilde{\xi}_j)| + \frac{\tilde{x}_i-\tilde{\xi}_j}{(\beta s_0/b_0)}\ln\left|\frac{(\mathbf{R}_{ij,r})_2 - (\beta s_0/b_0)(1+\underline{y}_r)}{(\mathbf{R}_{ij,r})_1 + (\beta s_0/b_0)(1-\underline{y}_r)}\right| \tag{10b}$$

$$\mathbf{I}_1(\underline{\xi}_j,\underline{y}_r) = \underline{y}_r + \tfrac{1}{2}\left\{(1-\underline{y}_r)^2\ln|(\mathbf{R}_{ij,r})_1 - (\tilde{x}_i-\tilde{\xi}_j)| - (1+\underline{y}_r)^2\ln|(\mathbf{R}_{ij,r})_2 - (\tilde{x}_i-\tilde{\xi}_j)| + \frac{\tilde{x}_i-\tilde{\xi}_j}{(\beta s_0/b_0)^2}[(\mathbf{R}_{ij,r})_2 - (\mathbf{R}_{ij,r})_1]\right\} \tag{10c}$$

and

$$(\mathbf{R}_{ij,r})_1 = \left[(\tilde{x}_i-\tilde{\xi}_j)^2 + \left(\frac{\beta s_0}{b_0}\right)^2(1-\underline{y}_r)^2\right]^{1/2} \tag{10d}$$

$$(\mathbf{R}_{ij,r})_2 = \left[(\tilde{x}_i-\tilde{\xi}_j)^2 + \left(\frac{\beta s_0}{b_0}\right)^2(1+\underline{y}_r)^2\right]^{1/2} \tag{10e}$$

which completes the correction terms since none are needed for the evaluation of Eq. (5d).

Numerical application of Eq. (6) to a wide variety of planforms, reduced frequencies ($k \sim 1$) and Mach numbers has shown that the values of the terms represented by Eqs. (8a) and (10a) are not nearly as important as the value of that from Eq. (7a). This is due primarily to the interdigitation of downwash and integration points which tends to minimize the

resulting error. If the magnitude of k is much greater than unity, say 5 or 10, it is expected that Eqs. (8a) and (10a) would become more important.

The integration points $(\underline{\xi}_j, \underline{\eta}_s)$ and the downwash points $(\underline{x}_i, \underline{y}_r)$ are defined as follows

$$\underline{\xi}_j = -\cos\left(\frac{2j-1}{2J+1}\pi\right) \qquad j = 1,2,\ldots J \tag{11a}$$

$$\underline{\eta}_s = -\cos\left(\frac{2s-1}{2S}\pi\right) \qquad s = 1,2,\ldots S \tag{11b}$$

$$\underline{x}_i = -\cos\left(\frac{2i}{2\bar{m}+1}\pi\right) \qquad i = 1,2,\ldots \bar{m} \tag{12a}$$

$$\underline{y}_r = -\cos\left(\frac{r}{2R+1}\pi\right) \qquad r = 1,2,\ldots R \tag{12b}$$

The relationships between J and $\bar{m}$ and S and R, such that interdigitation is maintained (see Fig. 1), are

$$J = \textit{Integer Value}\,[(\bar{m}+0.5)n_c]$$
$$n_c = 1,3,5,\ldots \tag{13a}$$

and

$$S = n_s(2R+1) \qquad n_s = 1,3,5,\ldots \tag{13b}$$

where the operation "Integer Value [ ]" refers to the truncated integer value of the real number inside the brackets.

This completes the necessary equations for the planar surface method for arbitrary planforms. The next section will present the equations for extension to wings with surfaces.

Extension to Wings with Control Surfaces

The most important ingredients for a stable collocation method that is applicable to wings with control surfaces are: 1) an adequate pressure function that accounts for the hinge line singularity without being too complicated; 2) an efficient means of integrating the kernel function-pressure function product; and 3) rules for choosing the correct number of functions and control points for any planform. The following discussion will present the first two ingredients whereas the last will be discussed in the following sections on numerical applications.

Control Surface Functions

The pressure function used in this method is derived from a "pseudo three dimensionalizing" of the exact two dimensional function. The form is similar to that given by Landahl[11] for steady flow and was first presented by Cunningham[3] as follows:

$$\Delta\bar{p}_{CSn}(\underline{\xi},\underline{\eta}) = \frac{4\rho U_\infty{}^2}{b(\underline{\eta})}\, s_0(1-\underline{\eta}^2)^{1/2}[g_0(\underline{\eta}) + g_1(\underline{\eta})(1+\underline{\xi}) + g_2(\underline{\eta})\underline{\xi}(1+\underline{\xi}) + \cdots]\varphi_{CSn}(\underline{\xi},\underline{\eta}) \tag{14a}$$

where

$$\varphi_{CSn}(\underline{\xi},\underline{\eta}) = \ln\left|\frac{\{[1-\underline{\xi}\underline{\xi}_{Cn} + (1-\underline{\xi}^2)^{1/2}(1-\underline{\xi}_{Cn}{}^2)^{1/2}]^2 + E_n{}^2\}^{1/2} - E_n}{[(\underline{\xi}-\underline{\xi}_{Cn})^2 + E_n{}^2]^{1/2} - E_n}\right| \tag{14b}$$

and

$$E_n = \begin{cases} \beta^2(\underline{\eta}-\underline{\eta}_{1n})(\underline{\eta}_{2n}-\underline{\eta}), & \underline{\eta} \geq 0 \\ -\beta^2(\underline{\eta}+\underline{\eta}_{1n})(\underline{\eta}_{2n}+\underline{\eta}), & \underline{\eta} < 0 \end{cases} \tag{14c}$$

The $g_n(\eta)$ functions are identical with those given in Eq. (3b). The values of $\underline{\xi}_{Cn}$, $\underline{\eta}_{1n}$ and $\underline{\eta}_{2n}$ are the locations of the hingeline, left-hand edge, and righthand edge of the nth control surface, respectively. The hingeline location may vary within certain restrictions as will be pointed out in the next section. Thus, a slightly non-constant-percent chord hingeline is permissible. The side edges at stations $\underline{\eta}_{1n}$ and $\underline{\eta}_{2n}$ must be streamwise; however, the function given in Eqs. (14) is applicable to either trailing edge or leading edge controls.

Wings with several control surfaces may be treated by rewriting Eq. (14a) as

$$\Delta\bar{p}_{CS}(\underline{\xi},\underline{\eta}) = \frac{4\rho U_\infty{}^2}{b(\underline{\eta})}\, s_0(1-\underline{\eta}^2)^{1/2}\Phi_{CS}(\underline{\xi},\underline{\eta}) \tag{15a}$$

where

$$\Phi_{CS}(\underline{\xi},\underline{\eta}) = [g_0(\underline{\eta}) + g_1(\underline{\eta})(1+\underline{\xi}) + \cdots]\varphi_{CS}(\underline{\xi},\underline{\eta}) \tag{15b}$$

$$\varphi_{CS}(\underline{\xi},\underline{\eta}) = \sum_{n=1}^{ICS}\varphi_{CSn}(\underline{\xi},\underline{\eta}) \tag{15c}$$

for ICS total controls per semispan. The correct number of $g_n(\eta)$ functions depends on ICS and whether the flow is steady or unsteady. For a single control in steady flow, only $g_0(\eta)$ is necessary, for unsteady flow, however, $[g_0(\eta) + g_1(\eta)(1+\underline{\xi})]$ must be used. For two or more trailing edge or leading edge controls only, usually the single control rule on functions is satisfactory. For a combination of leading and trailing edge controls, $g_0(\eta)$ and $g_1(\eta)$ must be used for steady flow and up to $g_2(\eta)$ or $g_3(\eta)$ should be used for unsteady flow.

In addition to the control surface pressure functions, the regular functions must be used as defined in Eqs. (3). A minimum number of two regular chordwise functions must be used for steady flow and three for unsteady flow. The final sum of regular and control surface chordwise functions is equal to the number of downwash points per chord. The number of spanwise functions are identical for regular and control surface distributions and are equal to the number of downwash chords.

Integration of the Control Surface Pressure Functions

The chordwise integration of the kernel function-pressure function product must account for the hingeline singularities of the following form

$$\ln|[(\underline{\xi}-\underline{\xi}_{Cn})^2 + E_n{}^2]^{1/2} - E_n|$$

for each control surface. Although the singularities exist only between $\underline{\eta}_{1n}$ and $\underline{\eta}_{2n}$ such that $E_n > 0$, it is necessary to assume that they exist in the chordwise integral at all span stations. In this manner, the transition from singular to nonsingular integral correction terms is consistent and well behaved.

The downwash for an arbitrary wing with control surfaces may be expressed as

$$\overline{\mathbf{W}}(\tilde{x},\tilde{y}) = \overline{\mathbf{W}}_R(\tilde{x},\tilde{y}) + \overline{\mathbf{W}}_{CS}(\tilde{x},\tilde{y}) \tag{16}$$

where $\overline{\mathbf{W}}_R(\tilde{x},\tilde{y})$ is given in Eq. (6). The control surface downwash function, $\overline{\mathbf{W}}_{CS}(\tilde{x},\tilde{y})$ is obtained by substituting $\Delta\bar{p}_{CS}(\underline{\xi},\underline{\eta})$ in Eq. (2). As a result, Eq. (6) may be rewritten as

$$\frac{\overline{\mathbf{W}}_{CS}(\tilde{x}_i,\tilde{y})}{4\rho U_\infty{}^2} = \frac{2\pi^2}{S(2J+1)}\sum_{s=1}^{S}\sum_{j=1}^{J}(1-\underline{\eta}_s{}^2)\times [g_0(\underline{\eta}_s)(1-\underline{\xi}_j) + g_1(\underline{\eta}_s)(1-\underline{\xi}_j{}^2) + \cdots]\times \left(\frac{1+\underline{\xi}_j}{1-\underline{\xi}_j}\right)^{1/2}\varphi_{CS}(\underline{\xi}_j,\underline{\eta}_s)\mathbf{K}(\tilde{x}_i-\tilde{\underline{\xi}}_j,\tilde{y}_r-\tilde{\eta}_s,k,M) +$$

$$\frac{2\pi^2 S}{2J+1}\sum_{j=1}^{J}[g_0(\underline{y}_r)(1-\underline{\xi}_j) + g_1(\underline{y}_r)(1-\underline{\xi}_j{}^2) + \cdots]\times \left[1+\frac{|\underline{x}_i-\underline{\xi}_j|}{\underline{x}_i-\underline{\xi}_j}\right]\left(\frac{1+\underline{\xi}_j}{1-\underline{\xi}_j}\right)^{1/2}\varphi_{CS}(\underline{\xi}_j,\underline{y}_r)e^{-ik(\tilde{x}_i-\tilde{\underline{\xi}}_j)} +$$

$$\left\{-\frac{\pi}{S}\sum_{s=1}^{s}\frac{(1-\underline{\eta}_s{}^2)}{(\underline{y}_r-\underline{\eta}_s)^2}\Psi_{GCS}(\underline{y}_r,\underline{\eta}_s) + \pi S\Psi_{GCS}(\underline{y}_r,\underline{y}_r) + ik\left(\frac{s_0}{b_0}\right)^2\Phi_{CS}(\underline{x}_i,\underline{y}_r)\Gamma(\tilde{x}_i,\tilde{y}_r) - \frac{k^2}{2}\left(\frac{S_0}{b_0}\right)^2\frac{2\pi}{2J+1}\sum_{j=1}^{J}\Omega_{CS}(\underline{\xi}_j,\underline{y}_r)\right\} \tag{17}$$

The correction terms are modified as follows

$$\Psi_{GCS}(\underline{y}_r,\underline{\eta}_s) = \sum_{p=0}^{1}[(-1)^p\Phi_{CS_{p(x)}}(\underline{x}_i,\underline{\eta}_s)\psi_{Rp}(\tilde{y}_r,\tilde{\eta}_s) - \sum_{n=1}^{ICS}\Phi_{KCS_{p(x)}}(\underline{\xi}_{Cn},\underline{\eta}_s)\psi_{CSnp}(\tilde{y}_r,\tilde{\eta}_s)] \quad (18a)$$

where $\psi_R(\tilde{y}_r,\tilde{\eta}_s)$ is identical to that defined in Eqs. (7d–7g). The hingeline singularity is accounted for by ψ_{CSnp} and is written as

$$\psi_{CSn0}(\tilde{y},\tilde{\eta}) = \frac{1}{2}\left[\mathbf{L}_0(\underline{\xi}_{Cn},\underline{\eta}) - \frac{2\pi}{2J+1}\sum_{j=1}^{J}(1-\underline{\xi}_j^2)^{1/2}\times \ln|[(\underline{\xi}_j-\underline{\xi}_{Cn})^2+E_n^2]^{1/2}-E_n|\right] \quad (18b)$$

$$\psi_{CSn1}(\tilde{y},\tilde{\eta}) = \frac{1}{2}\left[\mathbf{L}_1(\underline{\xi}_{Cn},\underline{\eta}) - \frac{2\pi}{2J+1}\sum_{j=1}^{J}(1-\underline{\xi}_j^2)^{1/2}\times (\underline{\xi}_j-\underline{\xi}_{Cn})\ln|[(\underline{\xi}_j-\underline{\xi}_{Cn})^2+E_n^2]^{1/2}-E_n|\right] \quad (18c)$$

where

$$\mathbf{L}_0(\underline{\xi}_{Cn},\underline{\eta}) = (1-\underline{\xi}_{Cn})\ln|[(1-\underline{\xi}_{Cn})^2+E_n^2]^{1/2}-E_n| + (1+\underline{\xi}_{Cn})\ln|[(1+\underline{\xi}_{Cn})^2+E_n^2]^{1/2}-E_n| - E_n\ln\left|\frac{\{[1+\underline{\xi}_{Cn})^2+E_n^2]^{1/2}-(1+\underline{\xi}_{Cn})\}\times\{[(1-\underline{\xi}_{Cn})^2+E_n^2]^{1/2}-(1-\underline{\xi}_{cn})\}}{E_n^2}\right| \quad (18d)$$

$$\mathbf{L}_1(\underline{\xi}_{cn},\underline{\eta}) = \underline{\xi}_{Cn} + \tfrac{1}{2}\{(1-\underline{\xi}_{cn})^2\ln|[(1-\underline{\xi}_{cn})^2+E_n^2]^{1/2}-E_n| - (1+\underline{\xi}_{Cn})^2\ln|[(1+\underline{\xi}_{Cn})^2+E_n^2]^{1/2}-E_n|\} - \tfrac{1}{2}E_n\{[(1-\underline{\xi}_{Cn})^2+E_n^2]^{1/2}-[1+\underline{\xi}_{Cn})^2+E_n^2]^{1/2}\} \quad (18e)$$

The hingeline correction terms are obtained by adding and subtracting the product of the kernel function and the multiplier on the pressure function singularity in the vicinity of the hingeline. The treatment is similar to that used to derive Eqs. (10), the correction term for the kernel function logarithmic singularity. Thus the Φ_{KCSn} function is expressed as

$$\Phi_{KCS0}(\underline{\xi}_{Cn},\underline{\eta}) = [g_0(\underline{\eta}) + g_1(\underline{\eta})(1+\underline{\xi}_{Cn}) + \cdots]\mathbf{K}(\tilde{x}-\underline{\xi}_{Cn},\tilde{y}-\tilde{\eta},k,M) \quad (18f)$$

$$\Phi_{KCS1}(\underline{\xi}_{Cn},\underline{\eta}) = \left[\frac{\partial}{\partial\underline{\xi}}\Phi_{KCS0}(\underline{\xi},\underline{\eta})\right]_{\underline{\xi}_{Cn}} \quad (18g)$$

likewise

$$\Phi_{CS0}(\underline{x},\underline{\eta}) = [g_0(\underline{\eta}) + g_1(\underline{\eta})(1+\underline{x}) + \cdots]\varphi_{CS}(\underline{x},\underline{\eta}) \quad (18h)$$

$$\Phi_{CS1}(\underline{x},\underline{\eta}) = \left[\frac{\partial}{\partial\underline{\xi}}\Phi_{CS0}(\underline{\xi},\underline{\eta})\right]_{\underline{x}} \quad (18i)$$

The Ω_{CS} function is simply

$$\Omega_{CS}(\underline{\xi}_j,\underline{y}_r) = \sum_{p=0}^{1}\left\{\frac{\partial^p}{\partial\underline{\eta}^p}\Phi_{CS}(\underline{\xi}_j,\underline{\eta})\right\}_{\underline{\eta}=\underline{y}_r} e^{-ik(\tilde{x}_i-\tilde{\xi}_j)}\left[\mathbf{I}_p(\underline{\xi}_j,\underline{y}_r) - \frac{\pi}{S}\sum_{s=1}^{S}(1-\underline{\eta}_s^2)^{1/2}(\underline{\eta}_s-\underline{y}_r)^p\ln|\mathbf{R}_{ij,rs}-(\tilde{x}_i-\tilde{\xi}_j)|\right] \quad (19)$$

where $I_p(\underline{\xi}_j,\underline{y}_r)$ is are as defined previously in Eqs. (10b–10e).

Numerical Usage of the Method

In this section, discussions will be presented on the application of the equations developed in the previous sections to practical problems.

Boundary Conditions

The relationship given by Eqs. (6, 16, and 17), between downwash and the pressure function coefficients, a_{nm}, is not sufficiently simplified to permit solving for the a_{nm} as a function of an input arbitrary downwash. Hence it must be broken up into an influence coefficient form as is standard practice.[1,2,3,7,8] The equations resulting from the requirement for satisfying tangential flow at the control points $(\tilde{x}_i,\tilde{y}_r)$ are arranged into matrix form, yielding

$$[(A_{nm})_{ir}]\{a_{nm}^{(t)}\} = -4\pi\rho U_\infty^2\left\{ik\frac{z_{ir}^{(t)}}{b_0} + \frac{\partial z_{ir}^{(t)}}{\partial x}\right\} \quad (20)$$

where

$z_{ir}^{(t)}$ = vertical displacement of the tth mode (positive down) at the point $(\tilde{x}_i,\tilde{y}_r)$.

Equation (20) is solved (or the $[(A_{nm})_{ir}]$ matrix is inverted and saved for future use) for the $\{a_{nm}^{(t)}\}$ coefficients, which may then be inserted into Eqs. (3) to compute the pressure amplitude at any point $(\underline{\xi},\underline{\eta})$. If the wing has control surfaces, the modes may include control surface motion and the corresponding type of pressure functions must be included. Since both the regular and control surface pressure functions have the same spanwise functions, the chordwise characteristics become the only distinguishing feature. Thus the total pressure function is constructed as

$$\Delta\bar{p}(\underline{\xi},\underline{\eta}) = \frac{4\rho U_\infty^2}{b(\underline{\eta})}s_0(1-\underline{\eta}^2)^{1/2}\left\{[g_0(\underline{\eta}) + g_0(\underline{\eta})(1+\underline{\xi}) + \cdots]\times\varphi_{CS}(\underline{\xi},\underline{\eta}) + [g_{JC+1}(\underline{\eta}) + g_{JC+2}(\underline{\eta})(1+\underline{\xi}) + \cdots + g_{\bar{m}-1}(\underline{\eta})\underline{\xi}^{\bar{m}-JC-2}(1+\underline{\xi})]\left(\frac{1-\underline{\xi}}{1+\underline{\xi}}\right)^{1/2}\right\} \quad (21)$$

where JC = total number of chordwise control surface pressure functions, $\bar{m}$ = total downwash points per chord and total number of all chordwise pressure modes. As an example, the problems shown in the next section were run with $JC = 1$ for steady flow and $JC = 2$ for unsteady flow. The total $\bar{m}$ ranged from 3 to 5, that is the number of regular functions varied from 2 to 3.

Optimum Downwash and Integration Point Arrays

If one chooses to use the standard set of interdigitated downwash and integration points, $n_c = 1$ and $n_s = 1$ in Eqs. (13), then the optimum array of control points are defined as given by Cunningham.[3,7] This rule is simply stated that a converged solution may be obtained if the following ratio is approximately satisfied

$$\left(\frac{NS}{NC}\right)_{\text{conv}} \leq 0.8\left[\frac{\beta AR}{\cos\Lambda_{m\text{root}}}\right] \quad (22)$$

where NS = number of downwash chords, NC = number of downwash points per chord, AR = aspect ratio, $\Lambda_{m\,\text{root}} = 0.5[|\Lambda_{LE\text{root}}| + |\Lambda_{TE\text{root}}|]$. That is, $\Lambda_{m\text{root}}$ is the average of the absolute values of the leading and trailing edge sweep angles at the root. The minimum number for NC can be as low as 2, however, it is recommended that it not be less than 3.

Since Eq. (22) actually governs integral convergence, if one chooses to use excess integration points then the rule must be changed slightly to

$$\left(\frac{NSI}{NCI}\right)_{\text{conv}} \approx 1.6\left[\frac{\beta AR}{\cos\Lambda_{m\text{root}}}\right] \quad (23)$$

where NSI and NCI are the total number of spanwise and chordwise integration stations, J and S, respectively.

The rules presented previously are applicable to wings with control surfaces with two restrictions. The first restriction is that the hingeline and ends of the control surface should fall along or near lines which are halfway between rows and chords of control points. That is no control point should be very close to the control surface boundaries. This is equivalent to the specification that finite element representations of wings with control surfaces must use panel edges to simulate the control surface boundaries. The second restriction is that no hingeline may cross a row of control points. The hingeline may be non-constant percent chord as long as it does not violate this restriction.

Comparison with Experiment and Other Theories

The application of the method to arbitrary wings without control surfaces has been presented previously in both steady[7] and unsteady[3] flow. It has been compared with several classic methods with the exception of the NASA method developed by Watkins, Woolston, and H. J. Cunningham.[12] An indirect comparison has been made with this method, however, through a comparison with Laschka's technique[3] which he has shown to give essentially the same results as the NASA method.[4] Therefore, further applications to planar wings will not be presented in this paper for sake of brevity.

Some preliminary results have been presented previously for application of the method to wings with control surfaces.[3] Although the technique still contained some bugs at that time, the results were quite encouraging. This success led to further refinements which finally evolved into the method presented in this paper. As a result, the following solutions as obtained with the new technique, use only the control and integration point arrays and pressure functions dictated by the rules established in the previous sections. The minimum number of integration points are always used in the chordwise direction which range from 3 to 5 in all cases. Results of the comparison with experimental data and other theories verify the accuracy of the final integration scheme and method of solution.

Shown in Fig. 2 is a solution for a swept tapered wing with a deflected trailing edge aileron in steady subsonic flow. The total number of downwash points used was 36 ($NC = 3$, $NS = 12$) with one chordwise control surface function and two

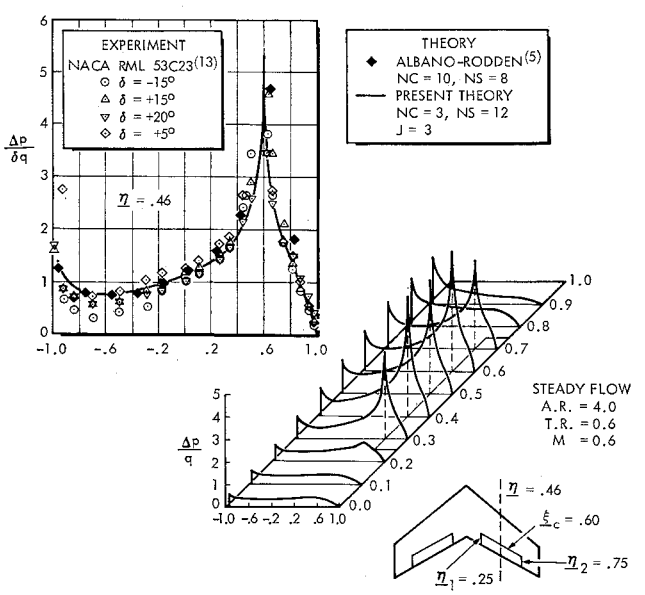

Fig. 2 Results for an aspect ratio 4.0 wing with a midspan aileron in steady flow.

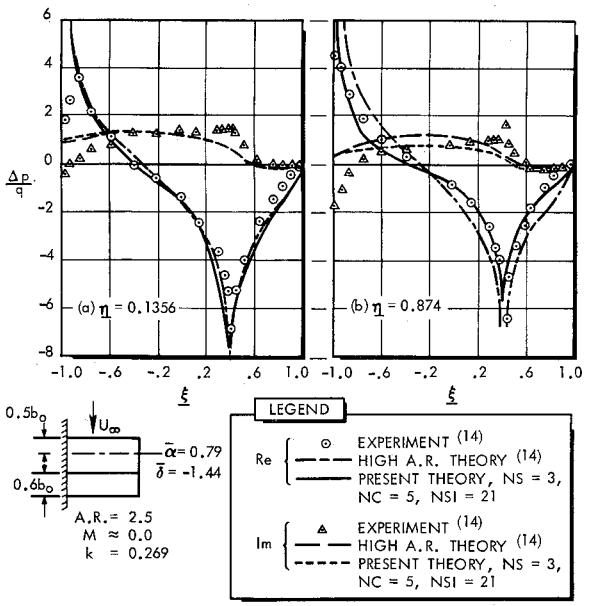

Fig. 3 Results for a rectangular wing with a control surface oscillating in a pitch and control surface mode.

regular pressure functions. Three integration points per chord were used. The results are compared with a large sampling of experimental data[13] and the 80 panel doublet lattice solution of Albano and Rodden.[5] The solution times on an IBM 360/65 were about 23 sec for the present method and about 60 sec for the doublet lattice method. At $\eta = 0.46$, the three way comparison is made where the two methods show essentially the same agreement with experiment forward of the hingeline. Aft of the hingeline, the present method is slightly superior to the doublet lattice method. (It should be noted that the doublet lattice solution shows better agreement with the same experimental data here than it does in the original reference.) Shown also in Fig. 2 is an over-all view of the pressure distribution on the wing. Although a comparison is not made here, the doublet lattice results at the other span stations show about the same agreement with the present method as is illustrated at $\eta = 0.46$.

In Fig. 3, results are shown for a rectangular wing oscillating in pitch about its quarter chord with an oscillating full span control surface.[14] The wing has an aspect ratio of 2.5; hence, a high aspect ratio type solution is quite applicable as was shown by Hertrich and Wagener[14] and here in the figure. The present method gives good results as is also shown, for a solution obtained with $NS = 3$, $NC = 5$, $NSI = 21$, and $NCI = 5$. Excess integration chords were used in this case to achieve a more economical solution since without them the convergence criteria would require $NS = 10$ for $NC = 5$. Thus it was possible to obtain a solution with fifteen control points for about 28 sec on the IBM 360/65. If fifty points were used, the solution time would be about 100 seconds. The types of chordwise functions used were two control surface and three regular functions.

In Fig. 4, results are shown for a lower aspect ratio swept tapered wing with an oscillating inboard aileron. The present method is compared with experimental data and the control surface method developed by Zwann.[15] The solution obtained with the present method used $NS = 7$ and $NC = 5$ with regular integration points and two control surface and three regular chordwise pressure functions. The present method took about 70 sec as compared to about 90 sec for a 56 panel doublet lattice solution, both on an IBM 360/65. The double lattice results are not shown for simplicity, but they compare with the present method in a manner similar to

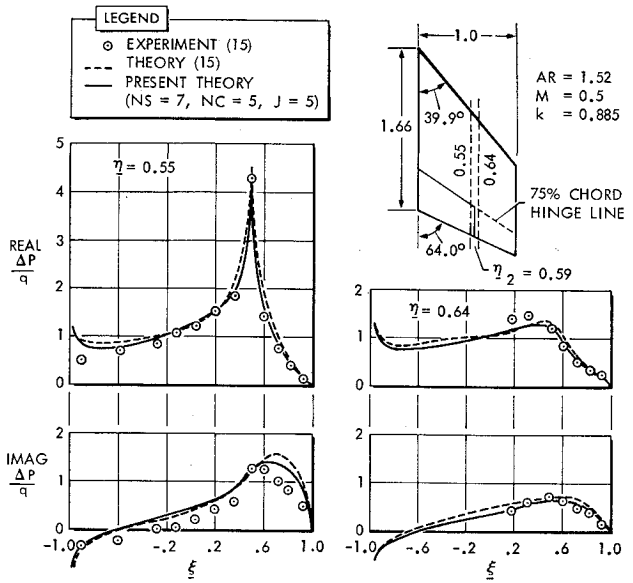

Fig. 4 Results for a swept-tapered wing with an oscillating inboard aileron.

that in Fig. 2. Both methods, however, tend to show slightly better agreement with the experimental data than the method of Zwaan.[15]

Conclusions

A stable and efficient collocation method has been developed for predicting oscillatory subsonic airloads on arbitrary wings with or without control surfaces. The method uses Gaussian quadrature integration with interdigitated downwash and integration points which leads to a highly efficient integration scheme. Correction terms are presented that account for errors incurred in the quadrature integration of the singularities that exist in the oscillatory subsonic kernel function and pressure functions assumed for control surfaces.

The rules developed for steady and unsteady flow over planar wings which define optimum downwash and/or integration point arrays, have been applied to wings with control surfaces. The only restrictions are that control points should straddle the control surface boundaries as much as possible and hinge lines must not cross rows of control points.

The method is verified by comparison with other theories and experimental data. On all configurations, the present method was shown to be more efficient than finite element methods for the same degree of accuracy. The margin of efficiency between the two approaches, however, was less for wings with controls as compared to planar wings results given in earlier references.

References

[1] Hsu, P. T., "Flutter of Low Aspect Ratio Wings, Part I, Calculation of Pressure Distributions for Oscillating Wings of Arbitrary Planform in Subsonic Flow by the Kernel-Function Method," Aeroelastic and Structures Research Lab. TR 64-1, Oct. 1957, MIT, Cambridge, Mass.

[2] Rowe, W. S., "Collocation Method for Calculating the Aerodynamic Pressure Distributions on Lifting Surfaces Oscillating in Subsonic Compressible Flow," AIAA Symposium on Structural Dynamics and Aeroelasticity, Boston, Mass., Aug. 30-Sept. 1, 1965, p. 31.

[3] Cunningham, A. M., Jr., "A Rapid and Stable Subsonic Collocation Method for Solving Oscillatory Lifting-Surface Problems by the Use of Quadrature Integration," *Materials and Structural Dynamics Volume, AIAA/ASME Eleventh Structures, Structural Dynamics, and Materials Conference*, AIAA, New York, 1970, pp. 1–16.

[4] Laschka, B., "Zur Theorie der harmonisch, schwingenden tragenden Fläche bei Unterschallströmung," *Zeitschrift für Flugwissenschaften* II, July 1963, pp. 265–291.

[5] Albano, E. and Rodden, W. P., "A Doublet-Lattice Method for Calculating Lift Distributions on Oscillating Surfaces in Subsonic Flows," *AIAA Journal*, Vol. 7, No. 2, Feb. 1969, pp. 279–285.

[6] Stark, V. J. E., "The Tangent Plane Method and Polar Coordinates—A New Approach in Lifting-Surface Theory," AIAA Paper 70–78, New York, 1970.

[7] Cunningham, A. M., Jr., "An Efficient, Steady, Subsonic Collocation Method for Solving Lifting-Surface Problems," *Journal of Aircraft*, Vol. 8, No. 3, March 1971, pp. 168–176.

[8] Cunningham, A. M., Jr., "On the Treatment of the Kernel Function Singularities in the Integral Equation of Unsteady Subsonic Lifting Surface Theory," Convair Aerospace Division of General Dynamics, ERR-FW-746, Aug. 1968.

[9] Watkins, C. E., Runyan, H. L., and Woolston, D. S., "On the Kernel Function of the Integral Equation Relating the Lift and Downwash Distributions of Oscillating Finite Wings in Subsonic Flow," Rept. 1234, 1955, NACA.

[10] Stroud, A. H. and Secrest, D., *Gaussian Quadrature Formulas*, Prentice-Hall, Englewood Cliffs, N.J., 1966.

[11] Landahl, M. T., "On the Pressure Loading Functions for Oscillating Wings with Control Surfaces," *Proceedings of the AIAA/ASME Eight Structures Structural Dynamics and Materials Conference*, Palm Springs, Calif., March 1967, pp. 142–147.

[12] Watkins, C. E., Woolston, D. S., and Cunningham, H. J., "A Systematic Kernel Function Procedure for Determining Aerodynamic Forces on Oscillating or Steady Finite Wings at Subsonic Speeds," TR-R-48, 1959, NASA.

[13] Hammond, A. D. and Keffer, B. M., "The Effect at High Subsonic Speeds of a Flap-Type Aileron on the Chordwise Pressure Distribution Near Mid-Semi-span of a Tapered 35° Sweptback Wing of Aspect Ratio 4 Having NACA 65A006 Section," RM L53C23, 1953, NACA.

[14] Hertrich, H. and Wagener, J., "Ein Verfahren zur Messung und automatischen Registrierung instationärer Druckverteilungen," Deutsche Luft-und Raumfahrt Forschungsbericht 67–54, June 1967.

[15] Bergh, H., Tijdeman, H., and Zwaan, R. J., "High Subsonic and Transonic Effects on Pressure Distributions Measured for a Swept Wing with Oscillating Control Surfaces," *Zeitschrift für Flugwissenschaften*, 18 Jahrgang, Heft 9/10, Sept./Oct. 1970, pp. 339–347.